

# Dynamic zonation of liver polyploidy

Sivan Tanami<sup>1</sup> · Shani Ben-Moshe<sup>1</sup> · Anat Elkayam<sup>1</sup> ·  
Avi Mayo<sup>1</sup> · Keren Bahar Halpern<sup>1</sup> · Shalev Itzkovitz<sup>1</sup>

Received: 17 December 2015 / Accepted: 4 May 2016  
© Springer-Verlag Berlin Heidelberg 2016

**Abstract** The liver is a polyploid organ, consisting of hepatocytes with one or two nuclei each containing 2, 4, 8 or more haploid chromosome sets. The dynamic changes in the spatial distributions of polyploid classes across the liver lobule, its repeating anatomical unit, have not been characterized. Identifying these spatial patterns is important for understanding liver homeostatic and regenerative turnover, as well as potential division of labor among ploidy classes. Here, we use single molecule-based tissue imaging to reconstruct the spatial zonation profiles of liver polyploid classes in mice of different ages. We find that liver polyploidy proceeds in spatial waves, advancing more rapidly in the mid-lobule zone compared to the periportal and perivenous zones. We also measure the spatial zonation profiles of S-phase entry at different ages and identify more rapid S-phase entry in the mid-lobule zone at older ages. Our findings reveal fundamental features of liver spatial heterogeneity and highlight their dynamic changes during development and aging.

**Keywords** Liver zonation · Liver polyploidy · Systems biology · Single molecule imaging · Stem cells

---

**Electronic supplementary material** The online version of this article (doi:10.1007/s00441-016-2427-5) contains supplementary material, which is available to authorized users.

---

✉ Shalev Itzkovitz  
shalev.itzkovitz@weizmann.ac.il

<sup>1</sup> Department of Molecular Cell Biology, Weizmann Institute of Science, Rehovot, Israel

## Introduction

The liver is a heterogeneous organ comprised of lobules which are polarized by blood flowing from portal nodes towards draining central veins. This polarization creates gradients of inputs such as oxygen, hormones and nutrients. As a result, hepatocytes that reside at the upstream periportal zone differ from hepatocytes in the downstream perivenous zone in the expression of key metabolic genes, a phenomenon termed ‘metabolic zonation’ (Gebhardt 1992; Jungermann and Keitzmann 1996; Braeuning et al. 2006; Colnot and Perret 2011). A second ubiquitous source of liver heterogeneity is its polyploidy (Celton-Morizur et al. 2009; Celton-Morizur and Desdouets 2010; Duncan et al. 2010; Pandit et al. 2012; Gentric and Desdouets 2014; Wang et al. 2014; Duncan 2013). Unlike most tissues, the liver is a mixture of hepatocytes that contain either one or two nuclei, each with either 2, 4, 8 or more haploid chromosome sets. While all hepatocytes have the capacity to divide (Bralet et al. 1994), liver homeostatic and regenerative turnover has been suggested to be preferentially fueled by diploid progenitors (Wang et al. 2015). The spatial location of these progenitors is still under debate (Font-Burgada et al. 2015; Wang et al. 2015).

In rodents, the liver is diploid at birth and becomes polyploid around weaning (Celton-Morizur et al. 2009). While the gradual increase in liver polyploidy during development and aging, predominantly through failed cytokinesis, is well documented (Epstein 1967; Celton-Morizur and Desdouets 2010; Gentric and Desdouets 2014), the dynamic changes in spatial zonation profiles of polyploid classes have not been characterized. To this end, we combined 3D imaging, single molecule detection of nascent mRNA and image processing to quantify the spatial zonation profiles of liver polyploid classes during development and aging.

## Materials and methods

All animal studies were approved by the Institutional Animal Care and Use Committee of WIS. C57bl6 male mice were fasted for 5 h before sacrifice by cervical dislocation and tissues were harvested and processed as previously described (Bahar Halpern et al. 2015). Tissues were stained with DAPI nuclear stain and phalloidin membrane stain. Cryosections 25  $\mu\text{m}$  thick were used for all experiments. Image stacks of 45 optical sections, with Z spacing of 0.3  $\mu\text{m}$  were acquired with a Nikon Ti-E inverted fluorescence microscope equipped with a  $\times 100$  oil-immersion objective and a Photometrics PIXIS 1024 CCD. The portal node was identified morphologically on DAPI images based on the bile ductule, and the central vein was identified using simultaneous single molecule fluorescence in situ hybridization (smFISH) for glutamine synthetase. Ploidy classification was based on the nuclear diameters of the maximal cross-sectional area of the hepatocyte nuclei and validated by smFISH for Pck1 (Bahar Halpern et al. 2015), a gene that exhibits abundant active transcription sites in the fasted state throughout the liver lobule. Continuous EdU incorporation was performed for 10 days on four 2-month-old mice and five 5-month-old mice. A full description is detailed in the [Supplementary Materials](#).

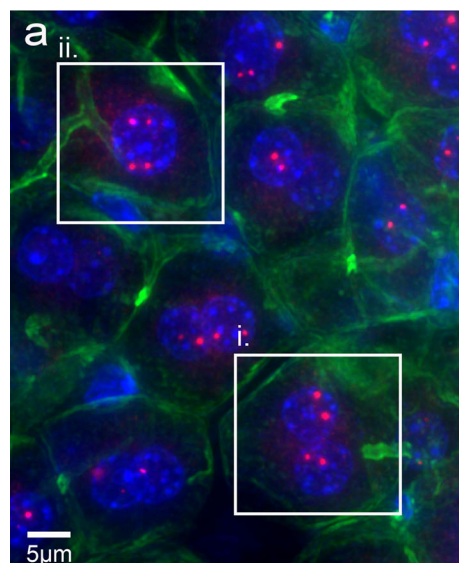


**Fig. 1** Method for quantifying liver polyploidy in situ. **a** Liver cross-section of a 2-month-old mouse stained with DAPI nuclear staining (blue), phalloidin cell-border staining (green) and smFISH for Pck1 (red dots). Boxes highlight a bi-nucleated tetraploid hepatocyte (i) containing two diploid nuclei and a mono-nucleated tetraploid hepatocyte (ii). Image is a maximal projection of 29 optical Z-sections. **b** Distribution of maximal nuclear diameters in liver cells measured in situ.

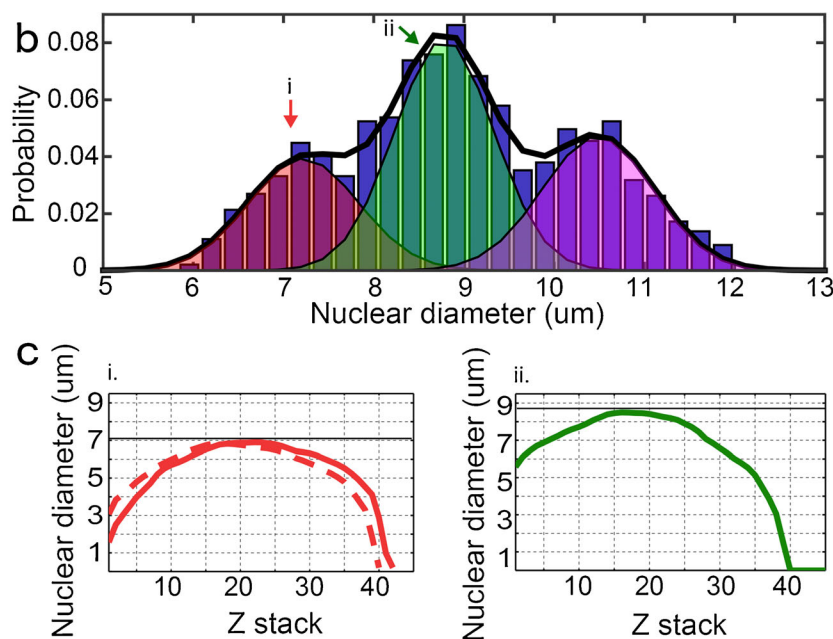
## Results

### Reconstruction of liver ploidy maps

We stained 25- $\mu\text{m}$  mouse liver cryosections with DAPI nuclear stain as well as phalloidin membrane stain. In addition, we used smFISH for glutamine synthetase (Glul), a gene that labels hepatocytes near the central vein, and bile ductule morphology to identify the portal nodes. We segmented individual hepatocytes spanning the lobule axis and generated the 3D profile of their nuclear cross-sections (Fig. 1a-c). The resulting distribution of maximal cross-sectional nuclear diameters was multimodal and well fitted by a mixture of Gaussians (Fig. 1b), the means of which increased by approximately  $2^{1/3}$ , as expected, since nuclear volume has been shown to scale linearly with ploidy (Martin et al. 2002). We next established thresholds for ploidy classification using detection of transcription sites of phosphoenolpyruvate carboxykinase 1 (Pck1; Fig. 1a), a gene that is transcriptionally active in more than 90 % of loci in the fasted state (Bahar Halpern et al. 2015). Classification error was estimated to be smaller than 8 % ([Supplementary Materials](#)).

### Hepatocytes become polyploid more rapidly at the mid-lobule zones

We next examined the spatial distribution of ploidy classes along the liver lobule radial axis. To this end, we



Colored overlaid curves are obtained from a Gaussian Mixture Model (black curve) and represent the expected distributions of nuclear diameters for diploid nuclei (red), tetraploid nuclei (green) and octoploid nuclei (magenta). Red and green arrows mark the maximal cross-sectional diameter of the nuclei of cells (i) and (ii) in (a). Data include 8700 nuclei pooled from 12 mice. **c** Profiles of the nuclear cross-sectional diameters of cells (i) and (ii) in (a) at different optical Z-sections

divided the porto-venous axis into eight lobule segments, numbered from the perivenous zone (segment 1) to the periportal zone (segment 8; note that our nomenclature differs from the traditional 3-zone classification scheme, in which zone 1 denotes the periportal zone and zone 3 denotes the perivenous zone; Fig. 2). We used the reconstructed ploidy maps (Fig. 2b) to extract ploidy zonation profiles, the probabilities of hepatocytes in each segment to belong to specific ploidy classes (Fig. 2c). We divided the number of hepatocytes belonging to each ploidy class in every segment by the total number of segmented

hepatocytes within that segment (Fig. 2b, c). We reconstructed these profiles for C57bl6 male mice at 8 different ages between 2 weeks and 12 months (Fig. 3; Table S1). We observed two phases distinguished by the rates of polyploidization. At 2 weeks, livers were predominantly diploid. Over the next 2 weeks, during the weaning transition, the fraction of diploid hepatocytes drastically decreased as higher ploidy classes emerged (Fig. 3a–c). At ages above 1 month, polyploidization rates dropped and polyploidization proceeded at a relatively constant rate (Fig. 3a–c).

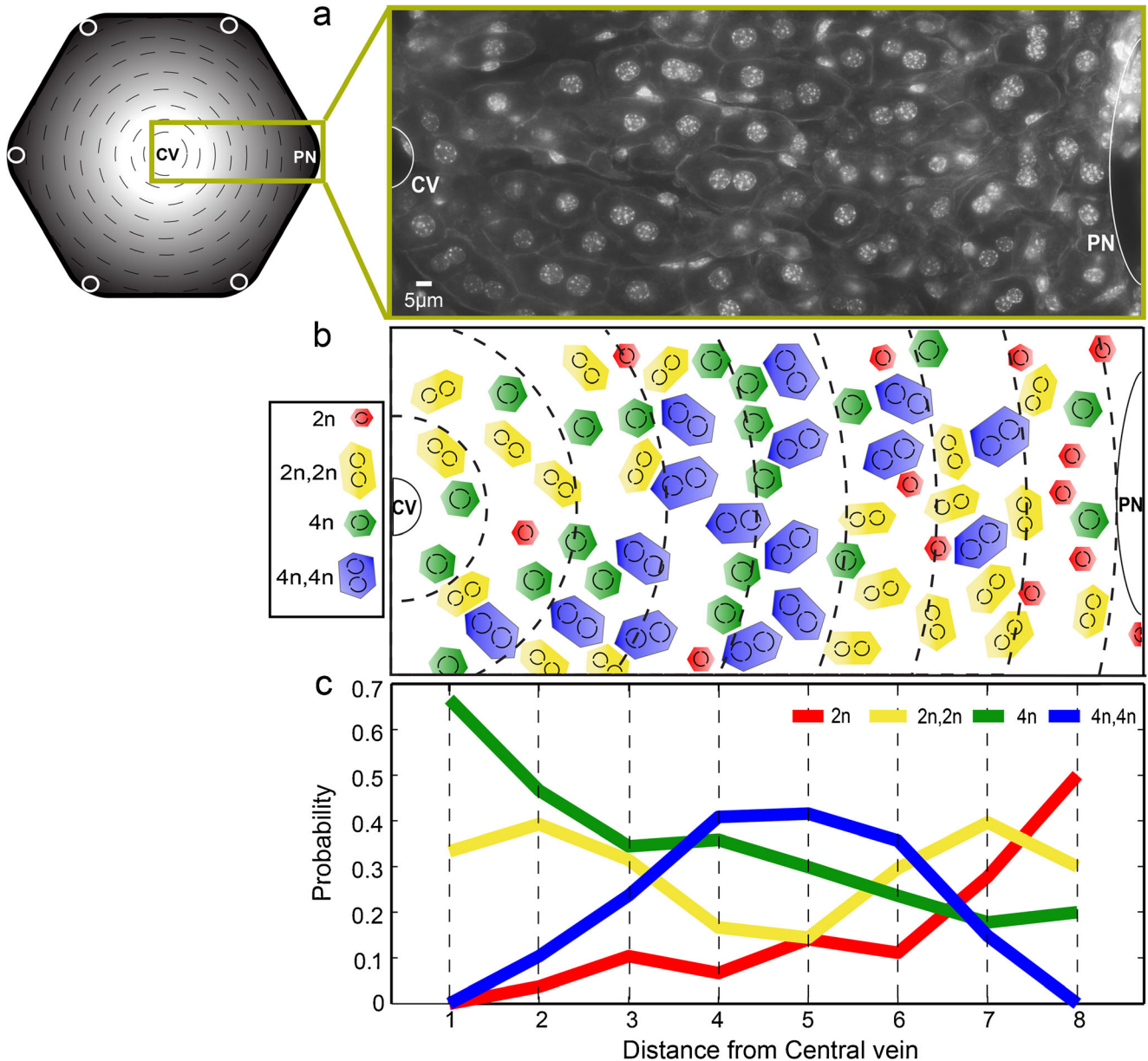
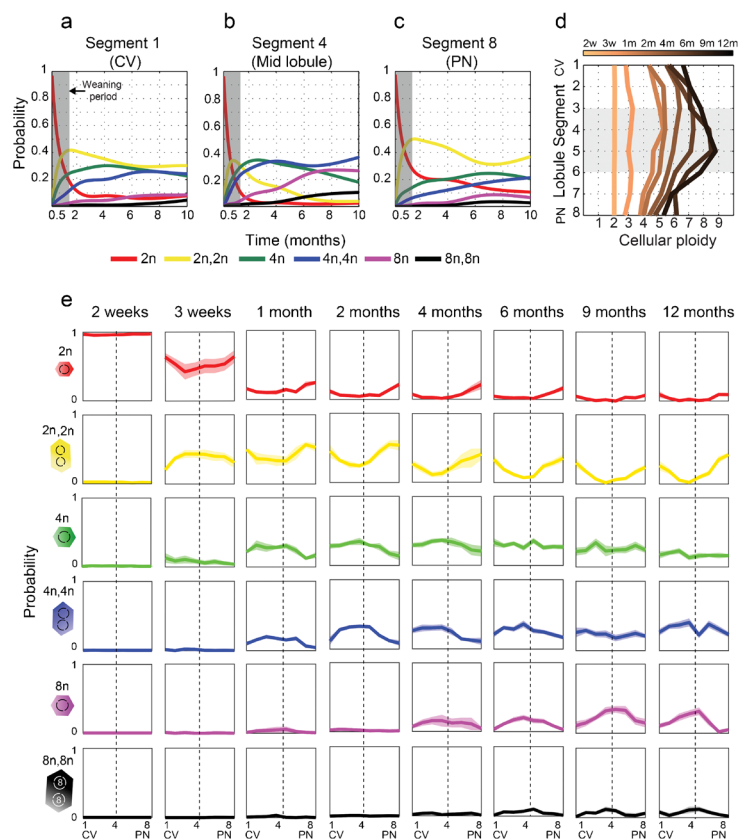


**Fig. 2** Liver polyloid maps. **a** Representative lobule cross-section from a 1-month-old mouse. *White contours* represent the central vein (CV) and portal node (PN). Image is a stacked combination of the DAPI and phalloidin channels. **b** Ploidy map of the lobule in (a). Hepatocytes are colored according to their ploidy class (*red* 2n; *yellow* 2n2n; *green* 4n;

*blue* 4n4n). The central vein contour was radially expanded at equal increments of 1/8 of the distance between the central vein and portal node (*dashed curves*). **c** Ploidy zonation profile of the map in (b). Each curve represents the fraction of segmented hepatocytes of a given ploidy class at each one of the eight lobule segments

**Fig. 3** Spatio-temporal dynamics of liver polyploidization. **a–c** Change in ploidy class abundance versus mouse age in lobule segments 1 (**a**), 4 (**b**) and 8 (**c**). **d**. Polyploidization proceeds most rapidly in the mid-lobule segments. Plotted are the averaged hepatocyte ploidy at different lobule segments (vertical axis) and different ages (increasingly dark shades). Gray box highlights the mid-lobule zone. **e**. Zonation profiles of ploidy classes at different ages. Y-axis shows the probability of a hepatocyte to belong to the plotted ploidy class, X-axis is the lobule segment. Patches represent the standard error of the means over all analyzed lobules for each age. Average profiles based on 20–47 lobules per age point, where at least 6 ploidy profiles are quantified for each mouse, 4 mice per age for younger ages (2 weeks to 4 months) and 2 mice per age for older ages (6–12 months)

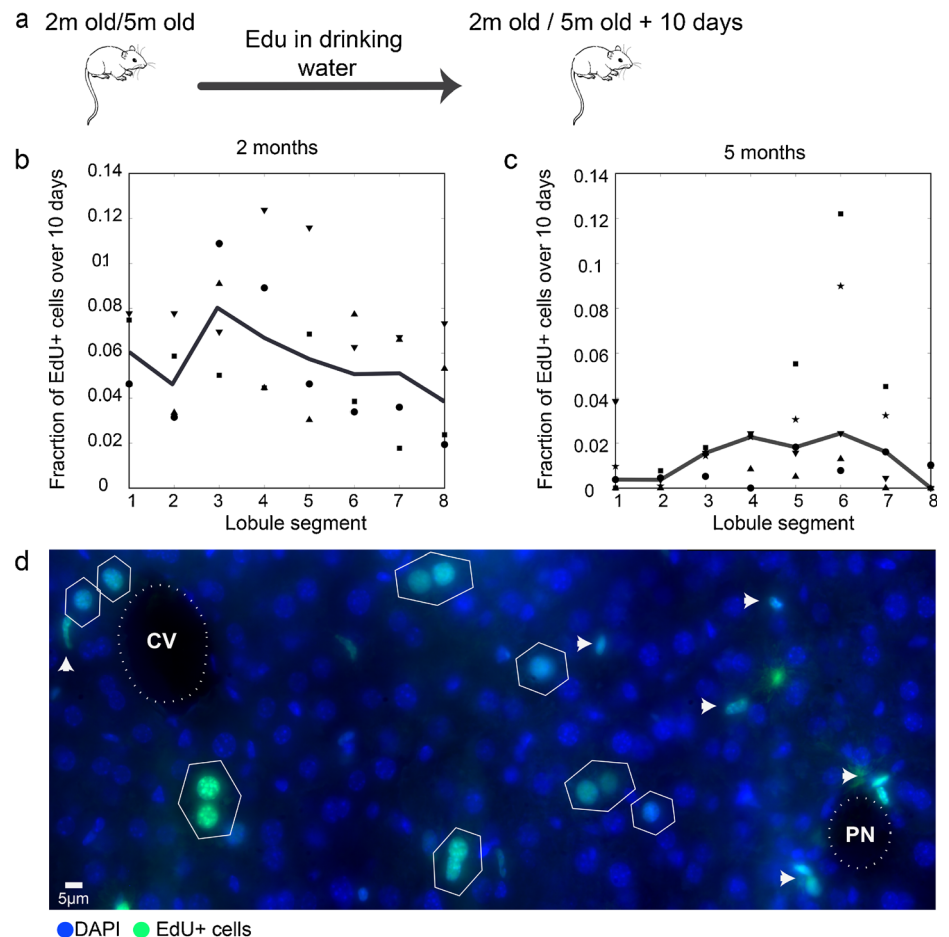


At the adult phase, over 1 month of age, we observed a sequential depletion of lower ploidy classes and subsequent increase in the higher classes (Fig. 3). Strikingly, this change was non-monotonic along the porto-venous axis. The mid-lobule zone (segments 4–5) progressed significantly faster to higher ploidy classes compared to the perivenous zone (segments 1–2) and periportal zone (segments 6–8) (Fig. 3d, e). For example, mono-nucleated octoploid hepatocytes (magenta curves, Fig. 3e) emerged at around age 6 months but were almost exclusively in the mid-lobule zones, reaching ~20 % of the hepatocyte population in segment 4 but less than 5 % in the perivenous segment 1 and periportal segment 8 (Wilcoxon rank sum  $P < 8 \times 10^{-5}$ ). Conversely, the tetraploid binucleated hepatocytes (yellow curve, Fig. 3e) were significantly depleted in the mid-lobule zone compared to the perivenous and periportal zones (7 % in segment 4 vs. 33 % in segments 1 and 35 % in segment 8, Wilcoxon rank sum  $P < 0.0025$ ). These results indicate that hepatocytes at different radial coordinates within the intact lobule form distinctly different subpopulations in terms of their polyploidization dynamics.

### Zonation patterns of S-phase entry rates

We next asked whether the non-monotonic zonation profiles of liver polyploidy might stem from increased turnover rates in the mid-lobule zone. S-phase entry is rare during normal liver physiology (Jones and Gores 1997; Duncan et al. 2010; Schmucker 2005), and thus cannot be robustly quantified using traditional staining techniques (Jones and Gores 1997; Kanzler and Galle 2000; Gujral et al. 2002; Schmucker 2005). To overcome this paucity of events, we supplemented drinking water with 5-ethynyl-2'-deoxyuridine (EdU) for a continuous pulse period of 10 days in 2-month-old mice and 5-month-old mice and measured the fraction of EdU+ cells at each lobule segment (Fig. 4). Our measurements revealed an intricate zonation pattern that varied with age. At 2 months of age, S-phase entry was uniform across the liver lobule (Kruskal–Wallis  $P = 0.502$ ). S-phase entry rate significantly decreased in 5-month-old mice (median of 0.01 at 5 months vs. 0.06 at 2 months, Wilcoxon rank sum  $P < 4E-9$ ). Interestingly, S-phase entry exhibited significant changes across the lobule segments in 5-month-old mice (Kruskal–

**Fig. 4** Zonation of EdU labeled cells. **a** Continuous EdU incorporation Experiment. **b, c** Zonation patterns of EdU labeling in 2-month-old mice (**b**) and in 5-month-old mice (**c**). Different shapes are means of the EdU fraction for each lobule segment in different mice over 8 analyzed lobules per mouse. *Line* denotes median of the biological repeats in each lobule segment. **d** An example of a lobule from a 2-month-old mouse demonstrating uniform spatial distribution of EdU+ cells across the lobule segments. *Scale bar* 5  $\mu$ m. EdU+ hepatocytes are segmented in *white*, *arrows* indicate EdU+ non-hepatocyte cells. *Blue* Dapi stain, *green* EdU labeling. *CV* central vein, *PN* portal node



Wallis  $P=0.043$ ), peaking at the mid-lobule segments (median S-phase entry rate of 0.0037 in segments 1–2 and 0.021 in segments 4–5, Wilcoxon rank sum  $P=0.023$ ). Thus, the higher S-phase entry rates at the mid-lobule zone may partially explain the non-monotonic zonation profile of liver polyploidization at older ages.

## Discussion

Our study revealed that liver polyploidization is non-random, but is rather highly structured. The non-monotonic spatial zonation profile of liver polyploidy uncovered here differs from all previously documented liver zonation patterns, such as those of gluconeogenesis, urea formation, glutamine synthesis, glycolysis and xenobiotic metabolism, all monotonically increasing or decreasing from the periportal to the perivenous zones (Gebhardt 1992; Jungermann and Keitzmann 1996; Braeuning et al. 2006). In contrast, we have found that the

zonation of polyploidy is non-monotonic, proceeding more slowly in both the periportal and perivenous zones. A recent study identified enrichment of polyploid hepatocytes in the mid-lobule zone in young mice (Morales-Navarrete et al. 2015). Our study extends these results to mice throughout development and aging, and uncovers the spatio-temporal dynamics of liver polyploidization. Liver homeostatic and regenerative turnover has recently been suggested to be preferentially fueled by diploid progenitors (Wang et al. 2015). It is interesting to note that our study identified a relatively higher abundance of diploid hepatocytes in both the perivenous and periportal zones, the putative sites of such progenitors (Font-Burgada et al. 2015; Wang et al. 2015).

The higher polyploidization rates we observed can be partially explained by our measured rates of S-phase entry, which peaked in the mid-lobule zone in 5-month-old mice. The relatively uniform patterns of S-phase entry in 2-month-old mice, however, suggest that additional proliferative features may be at play in shaping the polyploidization dynamics. Such features

include the probability for successful cytokinesis (Margall-Ducos et al. 2007), as well as ploidy-dependent death rates, which might spatially vary across the liver lobule at different ages. It will be important to characterize these features in future work to seek the mechanisms leading to the non-monotonic polyploidization patterns observed here.

Our measurements of the dynamic liver ploidy zonation profiles are important for interpreting large-scale gene expression studies aimed at understanding liver heterogeneity. Liver zonation and polyploidy are the key features that dictate the molecular identity of hepatocytes. Several studies analyzed differences in gene expression in different lobule zones (Gebhardt 1992; Jungermann and Keitzmann 1996; Braeuning et al. 2006) and in different ploidy classes (Lu et al. 2007). Our study emphasizes the importance of combining the information from both polyploidy and zonation when interpreting such large-scale gene expression screens. For example, highly polyploid hepatocytes would be expected to have lower expression levels of genes such as glutamine synthetase, since this gene is almost exclusively expressed at the perivenous zone, where we found polyploid cells to be less common. Our refined spatial analysis, which was carried out at higher spatial resolution compared to the traditional 3-zone classification, uncovered reproducible spatio-temporal waves of polyploidization. New techniques to globally interrogate individual cells while re-tracing them to their original tissue coordinate (Achim et al. 2015; Satija et al. 2015) will reveal specific metabolic functions of each of these segments. Our study provides the blueprint to stratify the results of such single-cell experiments according to ploidy state.

**Acknowledgments** We thank Shanie Landen for valuable comments on the manuscript. S.I. is supported by the Henry Chanoch Kreter Institute for Biomedical Imaging and Genomics, The Leir Charitable Foundations, Richard Jakubskind Laboratory of Systems Biology, Cymerman-Jakubskind Prize, The Lord Sieff of Brimpton Memorial Fund, The Human Frontiers Science Program, the I-CORE program of the Planning and Budgeting Committee and the Israel Science Foundation, the European Molecular Biology Organization Young Investigator Program and the European Research Council under the European Union's Seventh Framework Programme (FP7/2007-2013)/ERC grant agreement number 335122. S.I. is the incumbent of the Philip Harris and Gerald Ronson Career Development Chair.

## References

- Achim K, Pettit J-B, Saraiva LR et al (2015) High-throughput spatial mapping of single-cell RNA-seq data to tissue of origin. *Nat Biotechnol* 33:503–509. doi:10.1038/nbt.3209
- Bahar Halpern K, Tanami S, Landen S et al (2015) Bursty Gene Expression in the Intact Mammalian Liver. *Mol Cell* 58:147–156. doi:10.1016/j.molcel.2015.01.027
- Braeuning A, Itrich C, Köhle C et al (2006) Differential gene expression in periportal and perivenous mouse hepatocytes. *FEBS J* 273:5051–5061. doi:10.1111/j.1742-4658.2006.05503.x
- Bralet MP, Branchereau S, Brechot C, Ferry N (1994) Cell lineage study in the liver using retroviral mediated gene transfer. Evidence against the streaming of hepatocytes in normal liver. *Am J Pathol* 144:896–905
- Celton-Morizur S, Desdouets C (2010) Polyploidization of liver cells. *Adv Exp Med Biol* 676:123–135
- Celton-Morizur S, Merlen G, Couton D et al (2009) The insulin/Akt pathway controls a specific cell division program that leads to generation of binucleated tetraploid liver cells in rodents. *J Clin Invest* 119:1880–1887. doi:10.1172/JCI38677
- Colnot S, Perret C (2011) Liver zonation. In: Monga SPS (ed) *Molecular pathology of liver diseases*. Springer, New York, pp 7–16
- Duncan AW (2013) Aneuploidy, polyploidy and ploidy reversal in the liver. *Semin Cell Dev Biol* 24:347–356 doi:10.1016/j.semdb.2013.01.003
- Duncan AW, Taylor MH, Hickey RD et al (2010) The ploidy conveyor of mature hepatocytes as a source of genetic variation. *Nature* 467:707–710. doi:10.1038/nature09414
- Epstein CJ (1967) Cell size, nuclear content, and the development of polyploidy in the mammalian liver. *Proc Natl Acad Sci U S A* 57:327–334
- Font-Burgada J, Shalpour S, Ramaswamy S et al (2015) Hybrid Periportal Hepatocytes Regenerate the Injured Liver without Giving Rise to Cancer. *Cell* 162:766–779. doi:10.1016/j.cell.2015.07.026
- Gebhardt R (1992) Metabolic zonation of the liver: regulation and implications for liver function. *Pharmacol Ther* 53:275–354
- Gentric G, Desdouets C (2014) Polyploidization in liver tissue. *Am J Pathol* 184:322–331. doi:10.1016/j.ajpath.2013.06.035
- Gujral JS, Knight TR, Farhood A et al (2002) Mode of Cell Death after Acetaminophen Overdose in Mice: Apoptosis or Oncotic Necrosis? *Toxicol Sci* 67:322–328. doi:10.1093/toxsci/67.2.322
- Jones BA, Gores GJ (1997) Physiology and pathophysiology of apoptosis in epithelial cells of the liver, pancreas, and intestine. *Am J Physiol* 273:G1174–1188
- Jungermann K, Keitzmann T (1996) Zonation of Parenchymal and Nonparenchymal Metabolism in Liver. *Annu Rev Nutr* 16:179–203. doi:10.1146/annurev.nu.16.070196.001143
- Kanzler S, Galle PR (2000) Apoptosis and the liver. *Semin Cancer Biol* 10:173–184. doi:10.1006/scbi.2000.0318
- Lu P, Prost S, Caldwell H et al (2007) Microarray analysis of gene expression of mouse hepatocytes of different ploidy. *Mamm Genome* 18:617–626. doi:10.1007/s00335-007-9048-y
- Margall-Ducos G, Celton-Morizur S, Couton D et al (2007) Liver tetraploidization is controlled by a new process of incomplete cytokinesis. *J Cell Sci* 120:3633–3639. doi:10.1242/jcs.016907
- Martin NC, McCullough CT, Bush PG et al (2002) Functional analysis of mouse hepatocytes differing in DNA content: volume, receptor expression, and effect of IFN $\gamma$ . *J Cell Physiol* 191:138–144. doi:10.1002/jcp.10057
- Morales-Navarrete H, Segovia-Miranda F, Klukowski P et al (2015) A versatile pipeline for the multi-scale digital reconstruction and quantitative analysis of 3D tissue architecture. *eLife* 4, e11214. doi:10.7554/eLife.11214
- Pandit SK, Westendorp B, Nantasanti S et al (2012) E2F8 is essential for polyploidization in mammalian cells. *Nat Cell Biol* 14:1181–1191. doi:10.1038/ncb2585
- Satija R, Farrell JA, Gennert D et al (2015) Spatial reconstruction of single-cell gene expression data. *Nat Biotechnol* 33:495–502. doi:10.1038/nbt.3192
- Schmucker DL (2005) Age-related changes in liver structure and function: Implications for disease ? *Exp Gerontol* 40:650–659. doi:10.1016/j.exger.2005.06.009
- Wang M-J, Chen F, Li J-X et al (2014) Reversal of hepatocyte senescence after continuous in vivo cell proliferation. *HepatoL Baltim Md* 60:349–361. doi:10.1002/hep.27094
- Wang B, Zhao L, Fish M et al (2015) Self-renewing diploid Axin2(+) cells fuel homeostatic renewal of the liver. *Nature* 524:180–185. doi:10.1038/nature14863